

## Supporting Information for

# Stretchable Multifunctional Hydrogel for Sensing Electronics with Effective EMI Shielding Property

Mingming Hao,<sup>a,b</sup> Yongfeng Wang,<sup>b</sup> Lianhui Li,<sup>b</sup> Qifeng Lu,<sup>b</sup> Fuqin Sun,<sup>b</sup> Lili Li,<sup>b</sup> Xianqing Yang,<sup>b</sup> Yue Li,<sup>b</sup> Mengyuan Liu,<sup>b</sup> Sijia Feng,<sup>b</sup> Simin Feng,<sup>b</sup> and Ting Zhang<sup>\*a,b,c</sup>

<sup>a</sup>School of Nano Technology and Nano Bionics, University of Science and Technology of China, 96 Jinzhai Road, Hefei, Anhui, 230026, P. R. China

<sup>b</sup>i-lab, Key Laboratory of Multifunctional Nanomaterials and Smart Systems, Suzhou Institute of Nano-Tech and Nano-Bionics (SINANO), Chinese Academy of Sciences (CAS), 398 Ruoshui Road, Suzhou, Jiangsu 215123, P. R. China.

<sup>c</sup>Center for Excellence in Brain Science and Intelligence Technology, Chinese Academy of Sciences, Shanghai, 200031, P. R. China.

### Corresponding Author

\*E-mail: [tzhang2009@sinano.ac.cn](mailto:tzhang2009@sinano.ac.cn)

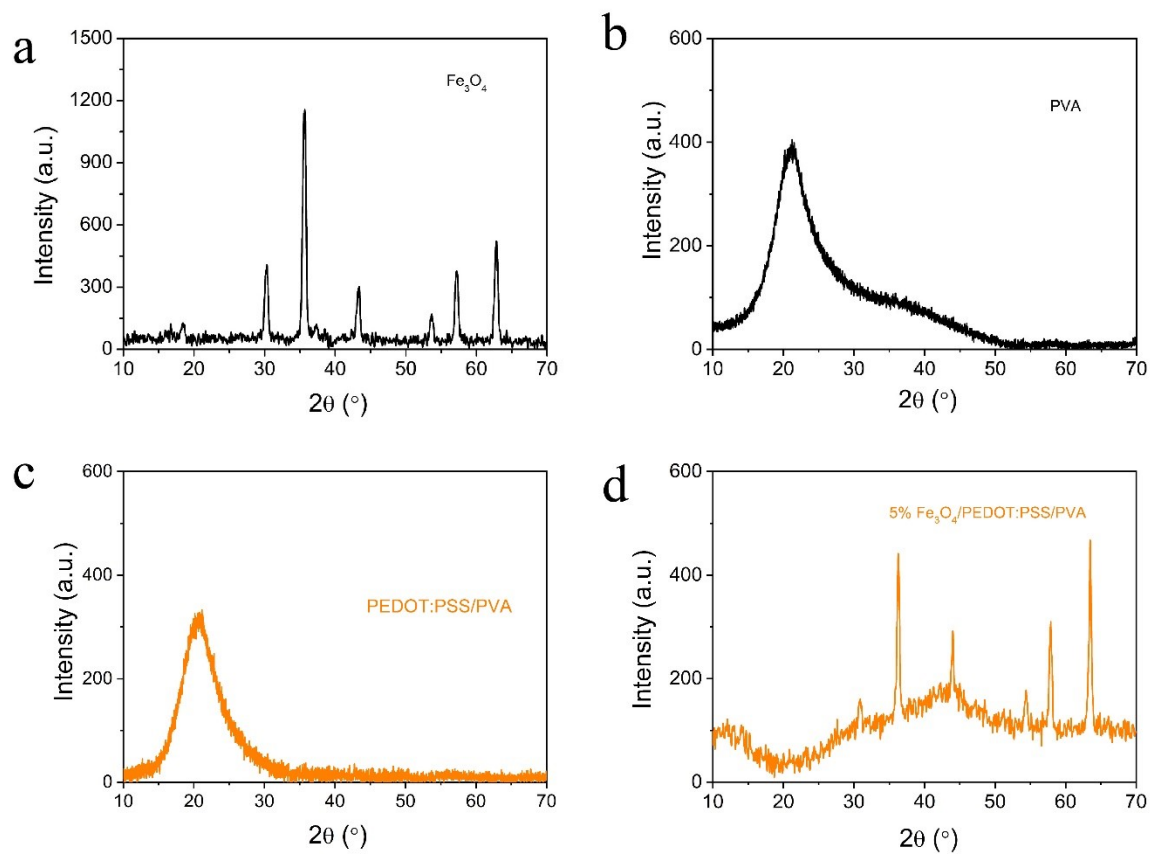


**Fig. S1.** XRD patterns of (a)  $\text{Fe}_3\text{O}_4$ , (b) PVA, (c) PEDOT: PSS/PVA, and (d) the 5%  $\text{Fe}_3\text{O}_4$ /PEDOT: PSS/PVA hydrogel, respectively.

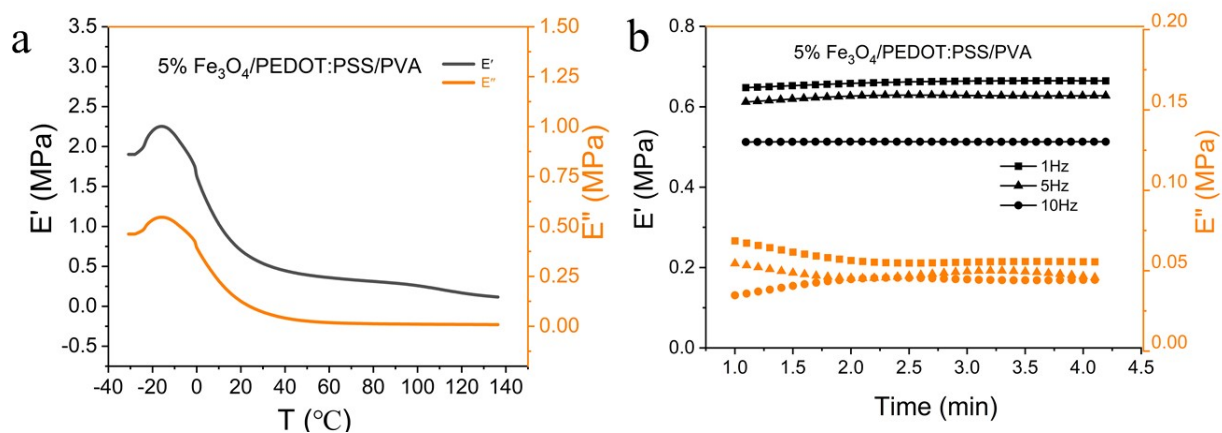


**Fig. S2.** (a) The dynamic mechanical analysis of the storage moduli (E') and loss moduli (E'') for the 5% Fe<sub>3</sub>O<sub>4</sub>/PEDOT: PSS/PVA as a function of temperature ranging from -45 to 125°C. (b) The dynamic mechanical analysis results of the storage moduli (E') and loss moduli (E'') of representative hydrogel 5% Fe<sub>3</sub>O<sub>4</sub>/PEDOT: PSS/PVA in 1 Hz, 5 Hz and 10 Hz.

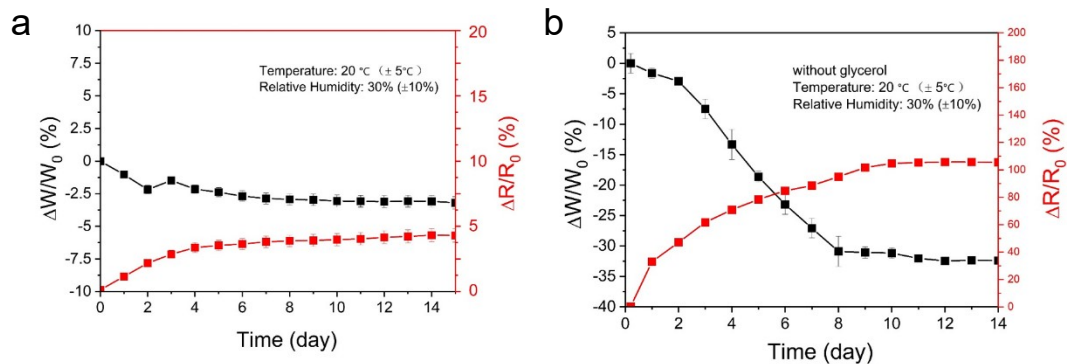


**Fig. S3.** The mass loss of the multifunction hydrogels with (a) and without glycerol (b) placed in ambient conditions at 20 °C ( $\pm 5$ ) and 30% ( $\pm 10\%$ ) humidity for 15 days. The relative resistance change ( $\Delta R/R_0$ ) of the multifunction hydrogel with (a) and without glycerol (b) placed in ambient conditions at 20 °C ( $\pm 5$ ) and 30% ( $\pm 10\%$ ) humidity for 14 days.

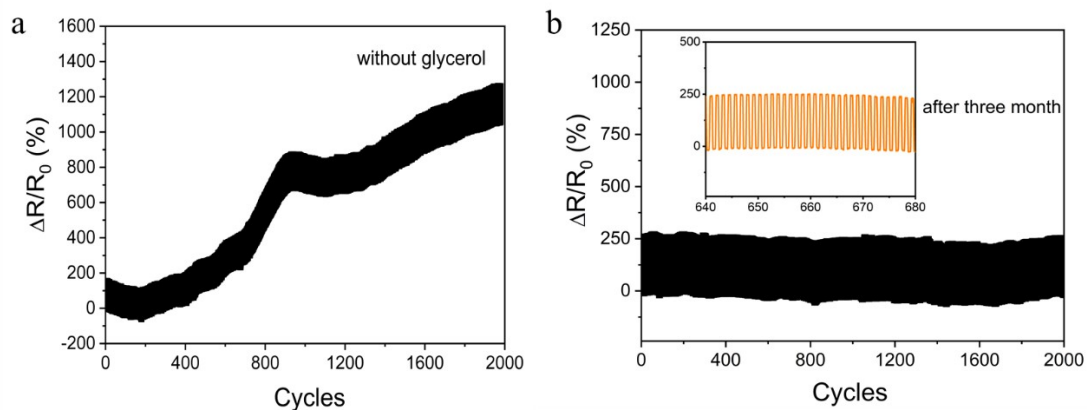


**Fig. S4.** (a) The resistance signal of the hydrogel without glycerol was observed in the detection of 2000 loading-unloading cycles. (b) The stable and reproducible response of 5%  $\text{Fe}_3\text{O}_4$ /PEDOT:PSS/PVA hydrogel was observed in the detection of 2000 loading-unloading cycles after three months.

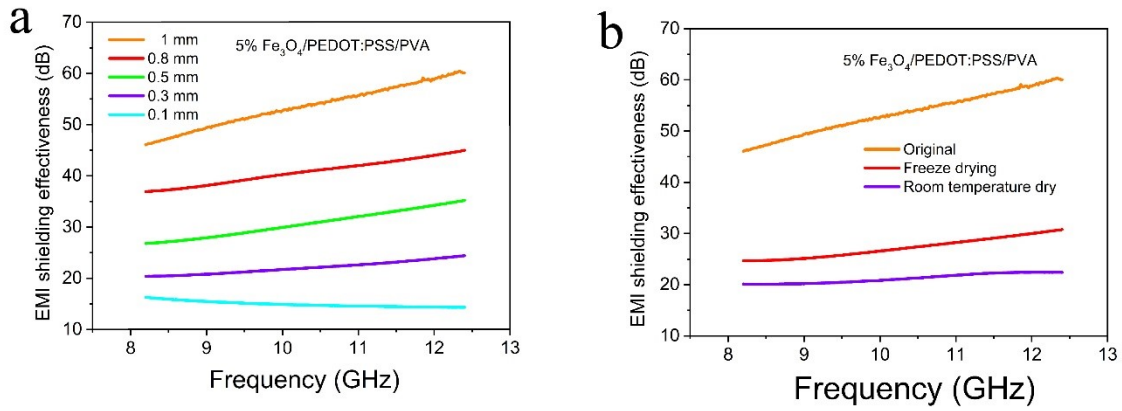


**Fig. S5.** (a) The EMI shielding effectiveness of 5%Fe<sub>3</sub>O<sub>4</sub>/PEDOT: PSS/PVA multifunction hydrogels films with different thicknesses. (b) The EMI shielding effectiveness of 5%Fe<sub>3</sub>O<sub>4</sub>/PEDOT: PSS/PVA multifunction hydrogels in a different state.

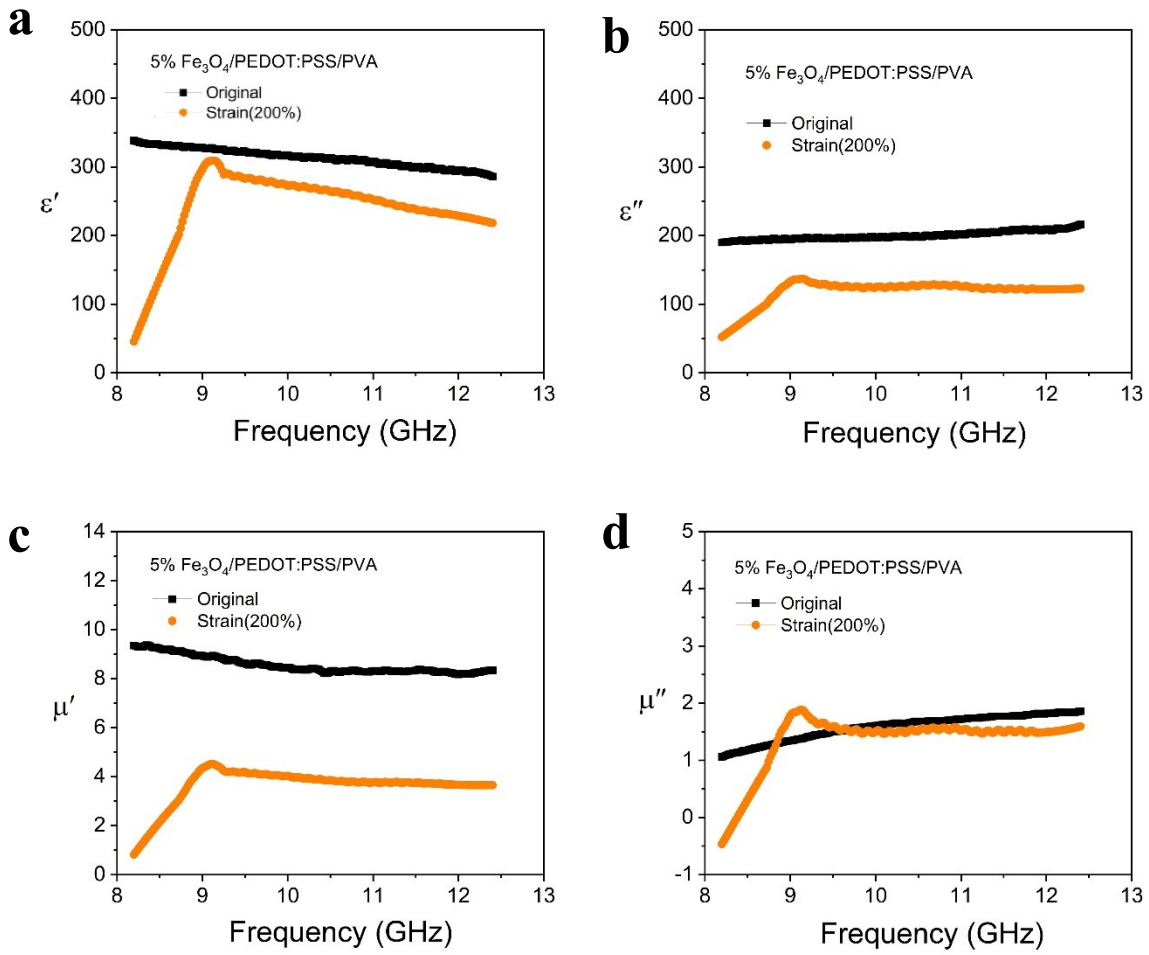


**Fig. S6.** (a-d) The relative complex permittivity and permeability of 5% Fe<sub>3</sub>O<sub>4</sub>/PEDOT: PSS/PVA multifunction hydrogels under the strain of 200%.

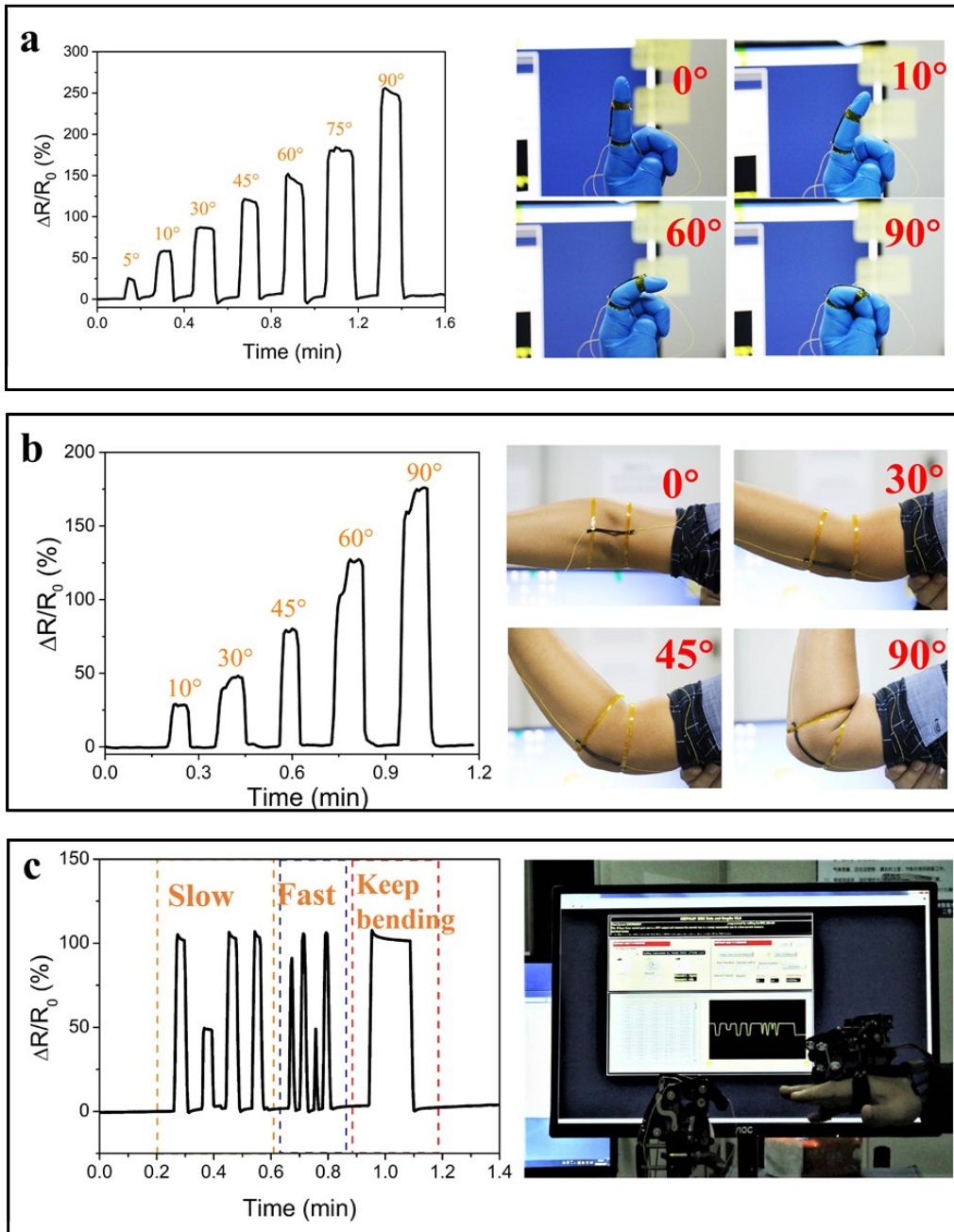


**Fig. S7.** The sensing performance of 5% Fe<sub>3</sub>O<sub>4</sub>/PEDOT: PSS/PVA multifunction hydrogels work as Figure (a) and elbow joint (b). c) The hydrogel sensor assembled on the mechanical finger to monitor the motion by the manipulator in real-time.



Video S1 and S2 show the self-recovery performance of the 5% Fe<sub>3</sub>O<sub>4</sub>/PEDOT: PSS/PVA hydrogel after repeated stretching and compression for ten cycles.

Video S3 shows the monitoring of the manipulator using the hydrogel-based wearable sensor.

Video S4 shows that the hydrogel-based wearable sensor can control the toy car remotely by assembling into a smart glove.